Development 138, 5147-5156 (2011) doi:10.1242/dev.067785

Gremlin 2 regulates distinct roles of BMP and Endothelin 1 signaling in dorsoventral patterning of the facial skeleton

Elizabeth Zuniga[1], Marie Rippen[1], Courtney Alexander[2], Thomas F. Schilling[2] and J. Gage Crump[1,*]

SUMMARY

Patterning of the upper versus lower face involves generating distinct pre-skeletal identities along the dorsoventral (DV) axes of the pharyngeal arches. Whereas previous studies have shown roles for BMPs, Endothelin 1 (Edn1) and Jagged1b-Notch2 in DV patterning of the facial skeleton, how these pathways are integrated to generate different skeletal fates has remained unclear. Here, we show that BMP and Edn1 signaling have distinct roles in development of the ventral and intermediate skeletons, respectively, of the zebrafish face. Using transgenic gain-of-function approaches and cell-autonomy experiments, we find that BMPs strongly promote *hand2* and *msxe* expression in ventral skeletal precursors, while Edn1 promotes the expression of *nkx3.2* and three Dlx genes (*dlx3b*, *dlx5a* and *dlx6a*) in intermediate precursors. Furthermore, Edn1 and Jagged1b pattern the intermediate and dorsal facial skeletons in part by inducing the BMP antagonist Gremlin 2 (Grem2), which restricts BMP activity to the ventral-most face. We therefore propose a model in which later cross-inhibitory interactions between BMP and Edn1 signaling, in part mediated by Grem2, separate an initially homogenous ventral region into distinct ventral and intermediate skeletal precursor domains.

KEY WORDS: BMP, Edn1, Gremlin 2, Jagged1, Notch, Craniofacial, Skeleton, Zebrafish, Dorsoventral patterning

INTRODUCTION

The facial skeleton develops from cranial neural crest cells (CNCCs) that populate a series of segments called the pharyngeal arches (Platt, 1893). Subsequently, skeletal elements of varying morphology develop from distinct DV domains within the arches (Crump et al., 2006; Eberhart et al., 2006), although a one-to-one correspondence between specific elements and DV expression domains has not been established. Initially, ventral CNCCs, unlike their dorsal counterparts, co-express *Hand2* and the Dlx family members *Dlx5* and *Dlx6* (Charite et al., 2001). As development progresses, DV gene expression becomes further segregated within the arches, with ventral CNCCs of zebrafish expressing *hand2*, intermediate CNCCs expressing *dlx3b*, *dlx5a*, *dlx6a* and *nkx3.2*, and dorsal CNCCs expressing *jag1b* (Talbot et al., 2010; Zuniga et al., 2010). Mice also show a similar separation of ventral *Hand2* and more intermediate *Dlx5/6* expression (Barron et al., 2011). An important issue is how such distinct preskeletal domains are specified during development.

All three classes of genes (Hand2, Dlx and Jag1b) are required to form distinct DV structures of the facial skeleton. Loss of *Hand2/hand2* function leads to reductions of the ventral skeleton and expansion of intermediate fates (Miller et al., 2003; Yanagisawa et al., 2003; Talbot et al., 2010), whereas Hand2 misexpression transforms the dorsal facial skeleton to a ventral morphology in mice (Sato et al., 2008). *Dlx5*$^{-}$; *Dlx6*$^{-}$ compound mutants display loss of ventral *Hand2* expression and transformation of the lower (ventral) jaw skeleton (Beverdam et al., 2002; Depew et al., 2002), and Dlx3b/4b/5a in zebrafish have important roles in development of the intermediate skeleton such as the jaw joint (Talbot et al., 2010). Similarly, reduction of Nkx3.2 in zebrafish causes joint fusions in the mandibular arch (Miller et al., 2003). Recent studies in zebrafish have also shown a prominent role for Jagged1b-Notch2 signaling in specifying the dorsal skeletal domain (Zuniga et al., 2010). Hence, at least in zebrafish, there is a clear functional separation between ventral, intermediate, and dorsal genes within the arches, and their disruption leads to specific craniofacial malformations.

Edn1 signaling specifies ventral and intermediate skeletal derivatives in the arches. Deficiencies in Edn1 or its receptors (Ednra in mouse and Ednra1/Ednra2 in zebrafish) result in reductions and/or dorsalization of the ventral and intermediate facial skeletons (Kurihara et al., 1994; Miller et al., 2000; Ozeki et al., 2004; Ruest et al., 2004; Nair et al., 2007). Cells lose expression of *Dlx3-6/dlx3-6*, *Hand2/hand2*, *Nkx3.2/nkx3.2*, *Msx1/msxe* and *epha4b* in the arches in *Edn1*$^{-/-}$ and *Ednra*$^{-/-}$ mouse mutants and *edn1*$^{-/-}$ zebrafish mutants (Miller et al., 2000; Ozeki et al., 2004; Ruest et al., 2004; Walker et al., 2006; Walker et al., 2007). Conversely, transgenic misexpression of Edn1 in mice or injection of human EDN1 protein in zebrafish transforms the dorsal skeleton (Kimmel et al., 2007; Sato et al., 2008). Edn1 also restricts Jagged1b-Notch2 activity to dorsal CNCCs in zebrafish, with loss of *jag1b* partially restoring ventral skeletal patterning in *edn1* mutants (Zuniga et al., 2010). Notably, the facial skeleton forms largely normally in the absence of both Edn1 and Jagged1b-Notch2 signaling, suggesting the presence of additional signals that promote ventral skeletal identity.

BMP signaling is likely to be one such pathway that plays a role in development of the ventral facial skeleton (reviewed by Nie et al., 2006). Members of the Bmp2/4/7 subfamily are expressed in the arches of mice, chickens and zebrafish (Francis-West et al., 1994; Wall and Hogan, 1995; Holzschuh et al., 2005; Liu et al., 2005). Furthermore, conditional deletion of Bmp4 in the arch epithelia of *Nkx2.5*^{CRE}*; Bmp4*$^{lacZ/flox}$ mice reduces *Hand2*, *Msx1* and *Msx2* expression in ventral CNCCs and reduces/transforms the ventral mandibular skeleton (Liu et al., 2004; Liu et al., 2005). However, gain-of-function BMP experiments have given

[1]Broad CIRM Center, University of Southern California Keck School of Medicine, Los Angeles, CA 90033, USA. [2]Department of Developmental and Cell Biology, University of California, Irvine, CA 92697, USA.

*Author for correspondence (gcrump@usc.edu)

Accepted 26 September 2011

conflicting results. In some cases, Bmp4-coated beads induce the formation of branched/duplicated Meckel's cartilages (Mina et al., 2002; Mariani et al., 2008), but in other cases they cause CNCC death and skeletal loss (Shigetani et al., 2000; Mariani et al., 2008). BMPs also function in many other facets of CNCC development, such as induction (Liem et al., 1995; Nguyen et al., 1998; Steventon et al., 2009), apoptosis (Graham et al., 1994), migration (Kanzler et al., 2000) and skeletogenesis (Wozney et al., 1988), which complicates the interpretation of these studies. A further obstacle is genetic redundancy among BMPs. In zebrafish, four members of the Bmp2/4/7 family – *bmp2a*, *bmp2b*, *bmp4* and *bmp7b* – are expressed in the developing pharyngeal arches (Holzschuh et al., 2005; Wise and Stock, 2010). As such, loss-of-function studies have yielded little insights into DV patterning roles of BMPs, with *bmp2b* mutants having gastrulation defects and a lack of neural crest (Nguyen et al., 1998), while *bmp4* mutants are viable and show no craniofacial defects (Wise and Stock, 2010). Here, we circumvent these issues by using zebrafish transgenic lines that allow us to control the timing and levels of BMP and Edn1 activity during craniofacial development. In so doing, we show that BMPs and Edn1 have distinct roles in establishing the ventral and intermediate domains of the arches, respectively.

Several types of BMP antagonists regulate BMP activity, indicating that precise levels of BMP signaling are crucial for developmental patterning. Early arch primordia in the mouse express *Noggin* and *Chordin*, and mutations in either BMP antagonist disrupts development of the ventral mandibular skeleton (Stottmann et al., 2001). By contrast, members of the Gremlin family of BMP antagonists, including *grem2* (*prdc1*) in zebrafish (Müller et al., 2006), are expressed in the arches at later stages (Hsu et al., 1998; Bardot et al., 2001). Functions for Gremlin proteins in craniofacial development have not been previously investigated. With gain- and loss-of-function analyses, we show that Grem2 promotes dorsal and intermediate skeletal fates by restricting BMP activity to the ventral arches. Edn1 and Jagged1b are also required for *grem2* expression, suggesting that they promote intermediate and dorsal skeletal fates in part through Grem2-mediated repression of BMP activity.

MATERIALS AND METHODS

Zebrafish lines

Zebrafish were staged as described previously (Kimmel et al., 1995). We used the following mutant and transgenic strains: *edn1*^{tf216b} (Miller et al., 2000), *jag1b*^{b1105} (Zuniga et al., 2010), *Tg(hsp70I:Gal4)*^{kca4} (Scheer and Campos-Ortega, 1999), *Tg(hsp70I:dnBmpr1a-GFP)*^{w30} (Pyati et al., 2005) and *Tg(BRE:*GFP*)* (Alexander et al., 2011). *Tg(UAS:Bmp4;cmlc2:GFP)*^{el49}, *Tg(UAS:Edn1;*α*-crystallin:Cerulean)*^{el249} and *Tg(UAS:Grem2;*α*-crystallin:Cerulean)*^{el326} transgenic lines were generated using Gateway Cloning (Invitrogen) and the Tol2kit (Kwan et al., 2007). Zebrafish *bmp4*, *edn1* and *grem2* cDNAs were amplified with the following primers: Bmp4-1F (5′-GGGGACAAGTTTGTACAAAA-AAGCAGGCTCGGCCACCATGATTCCTGGTAATCGAAT-3′), Bmp4-2R (5′-GGGGACCACTTTGTACAAGAAAGCTGGGTTTAGCGGCA-GCCACACCCCT-3′), Edn1-1F (5′-GGGGACAAGTTTGTACAA-AAAAGCAGGCTCGGCCACCATGCATTTGAGGATTATTTTCC-3′), Edn1-2R (5′-GGGGACCACTTTGTACAAGAAAGCTGGGTCTATG-AGTTTTCAGAAATCC-3′), Grem2FL-L (5′-GGGGACAAGTTTGTAC-AAAAAAGCAGGCTCGGCCACCATGAGCAGTAAGGTGGCGCT-3′) and Grem2FL-R (5′-GGGGACCACTTTGTACAAGAAAGCTGGG-TTCACTGTTTCCCCGACTCGGACA-3′). PCR products were combined with pDONR221 to generate pME-Bmp4, pME-Edn1 and pME-Grem2. pME-Bmp4 was combined with p5E-UAS, p3E-polyA and pDestTol2CG2 to generate *UAS*:Bmp4;*cmcl2*:GFP. pME-Edn1 and pME-Grem2 were combined with p5E-UAS, p3E-polyA and pDestTol2AB2 to generate *UAS*:Edn1;α-*crystallin*:Cerulean and *UAS*:Grem2;α-*crystallin*:Cerulean. pDestTol2AB2 is a modification of pDestTol2pA2 that contains an α-*crystallin* promoter driving lens Cerulean expression. Vectors were injected with transposase RNA and two independent stable lines were isolated for each, with *el49*, *el249* and *el326* being used for further analysis. In all experiments, genotyping of embryos confirmed the observed phenotypes. Genotyping for *jag1b*^{b1105}, *edn1*^{tf216b} and *hsp70I*:Gal4 are as described previously (Zuniga et al., 2010). The presence of *UAS*:Bmp4;*cmlc2*:GFP was confirmed by PCR with primers: cmcl2-L (5′-TGGTGCAGATGA-ACTTCAGG-3′) and cmcl2-R (5′-TGCTGGAATCTGAGCACTTG-3′). *UAS*:Edn1- and *UAS*:Grem2-positive embryos were selected based on lens Cerulean. For *hsp70I*:Gal4 experiments, *hsp70I*:Gal4-negative siblings served as controls.

Heat-shock treatments

For *hsp70I*:Gal4; *UAS*:Bmp4 and *hsp70I*:Gal4; *UAS*:Edn1 activations, embryos were placed in a programmable incubator at 40°C for 4-8 hours, as indicated, and then returned to 28.5°C. *hsp70I*:dnBmpr1a-GFP and *hsp70I*:Gal4; *UAS*:Grem2 embryos were placed in a thermocycler at 39°C from 16-17 hours post-fertilization (hpf) for heat-shock induction. For shorter *hsp70I*:Gal4; *UAS*:Bmp4 treatments, embryos were placed in 40°C pre-warmed embryo media at 21 hpf and transferred to 28.5°C embryo media after 1 or 3 minutes.

Morpholino injections

One-cell stage embryos were injected with 3 nl of *hand2*-morpholino (MO) (600 μM) (Maves et al., 2009), *grem2*-MO #1 (300 or 600 μM), or *grem2*-MO #2 (400 μM) (GeneTools, Philomath, OR, USA). *grem2*-MO #1 (5′-GACACAGCGCCACCTTACTGCTCAT-3′) and *grem2*-MO #2 (5′-CTCAGACACTGATGAAGGTGATGAT-3′) are translation blockers. Grem2:GFP was constructed by performing fusion PCR of the Grem2 cDNA template with primers Grem2:GFP-F (5′-GGGGACAAGTTT-GTACAAAAAAGCAGGCTCCACCATGAGCAGTAAGGTGGCGCTG-TGT-3′) and Grem2:GFP-1M (5′-ACAGCTCCTCGCCCTTGCTCACCA-TCTGTTTCCCCGACTCGGACACGCTC-3′) and the GFP template with primers Grem2:GFP-2M (5′-GAGCGTGTCCGAGTCGGGGAAACA-GATGGTGAGCAAGGGCGAGGAGCTG-3′) and Grem2:GFP-R (5′-GGGGACCACTTTGTACAAGAAAGCTGGGTTTACTTGTACAGCTC-GTCCATGC-3′). In the next round, the PCR product generated by Grem2:GFP-F and Grem2:GFP-R was combined with pDONR221 to generate pME-Grem2:GFP, which was combined with p5E-CMV/SP6, p3E-polyA and pDestTol2pA2 to generate *CMV/SP6*:Grem2:GFP:pA. After digestion with *Xho*I and *Bgl*II, mRNA was synthesized using the Ambion mMessage mMachine SP6 kit (Applied Biosystems/Ambion, Austin, TX, USA).

In situ hybridization and skeletal analysis

Skeletal staining and in situ hybridization are as described previously (Zuniga et al., 2010). *bmp4* and *grem2* probes were synthesized with T7 RNA polymerase from PCR products amplified with the following primers: Bmp4-L (5′-GTGAGGCGAACTCCTTTGAG-3′), Bmp4-R (5′-GCTAAT-ACGACTCACTATAGGTGTTTATCCGATGCAAACCA-3′), Grem2is-L (5′-AGTAAGGTGGCGCTGTGTCT-3′) and Grem2is-R (5′-GCTAATAC-GACTCACTATAGG-3′). All other probes are as described previously (Zuniga et al., 2010). Skeletal and colorimetric in situ hybridization images were acquired on a Leica D2500 upright microscope. Fluorescent images were captured on a Zeiss LSM5 confocal microscope using ZEN software and presented as sections or flattened projections as indicated. Levels were adjusted in Adobe Photoshop CS4, with identical adjustments applied to images from the same dataset.

Cell transplantation

Tissue transplantations were performed as described (Crump et al., 2004). Briefly, donor cells from *hsp70I*:dnBmpr1a-GFP or *fli1a*:GFP embryos were transplanted into the CNCC precursor domain of wild-type 6 hpf hosts, and hosts were subjected to heat-shock induction from 16-17 hpf. Fluorescent in situ hybridization was performed first with *dlx3b*, *msxe* or *hand2* probes, followed by immunohistochemistry (Crump et al., 2004) using 1:1000 rabbit polyclonal anti-GFP primary antibody (Torrey Pines Biolabs, East Orange, NJ, USA) and 1:300 AlexaFluor488 goat anti-rabbit secondary antibody (Invitrogen).

Statistical analysis

Using JMP 7.0 software, a Tukey-Kramer HSD test (α=0.05) was employed to show significance between multiple classes.

RESULTS

Bmp4 and Edn1 are expressed in non-overlapping domains of ventral arch ectoderm

Whereas previous studies have shown that *bmp2a*, *bmp2b*, *bmp4* and *bmp7b* are expressed in or around the pharyngeal arches of zebrafish (Holzschuh et al., 2005; Wise and Stock, 2010), their expression relative to developing CNCCs had not been thoroughly characterized. Here, we found that *bmp4* expression was restricted to ventral arch ectoderm at 24 hpf (Fig. 1A) and became localized to two domains of ventral ectoderm in the anterior mandibular and posterior hyoid arches at 36 hpf (Fig. 1D). Interestingly, *edn1* expression also localized to ventral arch ectoderm at these stages (Fig. 1B,E), but did so in a slightly more dorsal domain that did not overlap with *bmp4* expression (Fig. 1C,F). These distinct expression domains may indicate distinct roles in DV skeletal patterning.

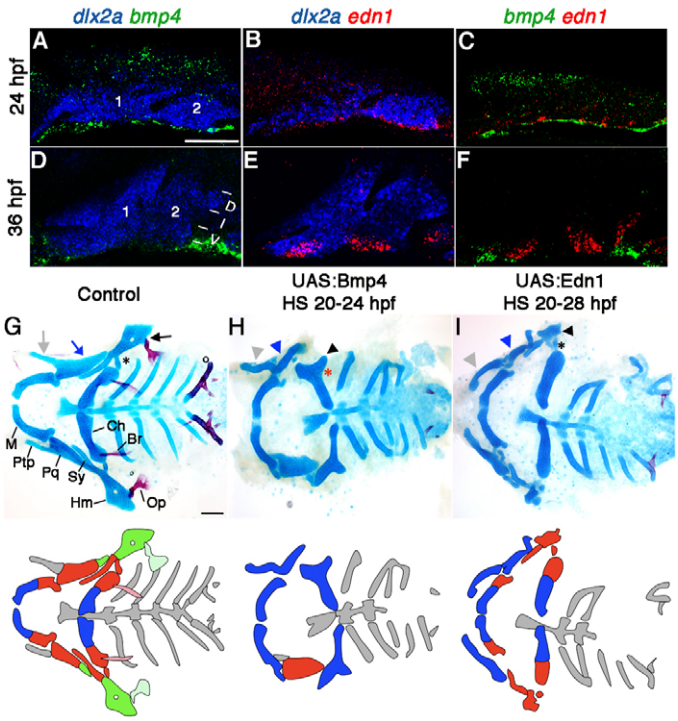

Fig. 1. Facial skeletal defects upon Bmp4 or Edn1 misexpression. (**A-F**) Confocal projections of in situ hybridization for *dlx2a* (blue), *bmp4* (green) and *edn1* (red) at 24 hpf (A-C) and 36 hpf (D-F) in wild type. Mandibular (1) and hyoid (2) arches are labeled, as well as dorsal (D), intermediate (I) and ventral (V) domains. (**G-I**) Ventral views (top) and schematics (below) of 5 dpf facial skeletons in control *hsp70I*:Gal4 (G) and *hsp70I*:Gal4; *UAS*:Bmp4 larvae subjected to a 4-hour heat-shock (H), and *hsp70I*:Gal4; *UAS*:Edn1 larvae subjected to an 8-hour heat-shock (I). Cartilage is blue and bone red. Schematics show dorsal (green), intermediate (red) and ventral (blue) regions with dermal bones lightly shaded. Hm (black arrow), Pq (blue arrow) and Ptp (grey arrow) were transformed (arrowheads) in *UAS*:Bmp4 and *UAS*:Edn1 larvae. In the intermediate second arch, the joint (asterisk) and symplectic bone were lost in *UAS*:Bmp4 but not *UAS*:Edn1 larvae. M, Meckel's cartilage; Pq, palatoquadrate cartilage; Ptp, pterygoid process; Sy, symplectic cartilage; Hm, hyomandibular cartilage; Ch, ceratohyal cartilage; Op, opercular bone; Br, branchiostegal ray bone. Scale bars: 50 μm.

Distinct effects of Bmp4 and Edn1 misexpression on facial skeleton development

To test the relative roles of Bmp4 and Edn1 in arch development, we took a gain-of-function approach. We created transgenic lines (*UAS*:Bmp4 and *UAS*:Edn1) in which zebrafish Bmp4 or Edn1 are expressed under the control of the Gal4-sensitive *UAS* promoter. In embryos doubly transgenic for these *UAS* lines and the heat-shock-inducible *hsp70I*:Gal4 vector (Scheer and Campos-Ortega, 1999), the timing and dose of Bmp4/Edn1 is regulated by the stage and duration of heat-shock treatment. Strikingly, *Tg*(*hsp70I:Gal4; UAS:Bmp4*) embryos (referred to as *UAS*:Bmp4) subjected to heat-shock at postmigratory CNCC stages (20-24 hpf), had a range of defects in the dorsal and intermediate skeletons (Fig. 1H, Table 1;

Table 1. Facial skeletal defects in *UAS*:Bmp4 and *UAS*:Edn1 zebrafish larvae

	Control	*UAS*:Bmp4	*UAS*:Edn1
First arch-derived elements			
Pq: (D-I)			
Unaffected	100%	55%	10%
Shape change	0%	45%	90%
Ptp: (Mx)			
Unaffected	100%	55%	10%
Shape change	0%	45%	90%
M-Pq joint: (I)			
Unaffected	100%	55%	100%
Absent	0%	**45%**	**0%**
M: (V-I)			
Unaffected	100%	55%	100%
Slightly reduced	0%	**45%**	**0%**
Second arch-derived elements			
Hm: (D)			
Unaffected	100%	16%	10%
Shape change	0%	84%	90%
Op: (D)			
Unaffected	100%	16%	10%
Shape change	0%	39%	0%
Absent	0%	45%	90%
Sy: (I)			
Unaffected	100%	16%	63%
Reduced	0%	39%	37%
Absent	0%	**45%**	**0%**
Hm-Ch joint: (I)			
Unaffected	100%	16%	100%
Absent	0%	**84%**	**0%**
Ch: (V-I)			
Unaffected	100%	55%	100%
Slightly reduced	0%	**45%**	**0%**
Br: (I)			
Unaffected	100%	55%	10%
Shape change	0%	0%	0%
Absent	0%	45%	90%

Percentage of animals showing defects. Arch-derived domains such as dorsal (D), intermediate (I), ventral (V) and maxillary (Mx) are listed next to each element. Intermediate-derived elements affected in *UAS*:Bmp4 but not *UAS*:Edn1 larvae are in bold. Animals displaying severe loss of the facial skeleton were not included. *hsp70I*:Gal4 animals subjected to the same heat-shock conditions were used as controls.

supplementary material Fig. S1), consistent with those induced by BMP4/7 beads (Alexander et al., 2011). Phenotypic variability was reflected in different levels of BMP activation as revealed by *bmp4* expression and a BMP-response-element:GFP (*BRE*:GFP) transgenic line (Alexander et al., 2011) (supplementary material Fig. S1). Previous fate mapping and gene expression studies have shown that in the mandibular arch: (1) dorsal CNCCs generate the posterior portion of the palatoquadrate (Pq) cartilage; (2) intermediate CNCCs form the jaw joint and joint-proximal regions of Pq and Meckel's (M) cartilage; and (3) ventral CNCCs form the majority of M. In the hyoid arch: (1) dorsal CNCCS form the hyomandibular (Hm) cartilage and opercle (Op) bone; (2) intermediate CNCCs form the symplectic (Sy), the joint, branchiostegal ray (Br) bones, and joint-proximal regions of ceratohyal (Ch) cartilage; and (3) ventral CNCCs form the majority of Ch (Fig. 1G). Defects in BMP-overexpressing embryos were most striking in the hyoid arch, where the dorsal Hm was typically transformed and fused in a mirror-image pattern to the ventral Ch, and intermediate Sy and joints were lost (Fig. 1H). In less severe classes, the dorsal Op bone was transformed to resemble the more ventral Br bone to which it fused (supplementary material Fig. S1F). In the mandibular arch, Pq and its Ptp process (a maxillary-derived element) became rod-shaped and resembled the ventral M, and the jaw joint was occasionally lost. *hsp70I*:Gal4-only siblings lacking the *UAS*:Bmp4 transgene but subjected to the same heat-shock treatment were unaffected (Fig. 1G). In addition, a few more severely affected *UAS*:Bmp4 animals displayed widespread loss of the facial skeleton and increased CNCC death (supplementary material Fig. S2).

We next compared the effect of Edn1 misexpression with the skeletal transformations seen with Bmp4 misexpression. In *Tg(hsp70I:Gal4; UAS:Edn1)* embryos subjected to a 20-28 hpf heat-shock treatment (referred to as *UAS*:Edn1), we observed dorsal-to-ventral transformations, similar to those reported for 20 hpf injection of human EDN1 protein into zebrafish arches (Kimmel et al., 2007). In particular, *UAS*:Edn1 larvae displayed defects in the dorsal Hm (arch 2) and Pq (arch 1) cartilages (Fig. 1I and Table 1). In addition, the maxillary-derived Ptp was thickened to resemble ventral M, similar to effects of ectopic BMPs. However, in marked contrast to Bmp4 misexpression, Edn1 misexpression never altered the intermediate-domain-derived joints or Sy in the hyoid arch. Hence, whereas Bmp4 misexpression affects development of both the dorsal and intermediate regions of the facial skeleton, Edn1 misexpression defects are largely confined further dorsally.

Distinct effects of Bmp4 and Edn1 misexpression on DV gene expression

We next asked whether misexpression of Bmp4 and Edn1 has distinct effects on DV gene expression. Strikingly, Bmp4 misexpression strongly upregulated expression of *hand2* throughout arch CNCCs at 36 hpf (Fig. 2B,G), whereas Edn1 misexpression slightly reduced *hand2* expression (Fig. 2C,H). By contrast, expression of the intermediate genes *dlx3b*, *dlx5a* and *dlx6a* was expanded throughout arch CNCCs of all *UAS*:Edn1 embryos, yet was variably reduced or mosaically expanded in different *UAS*:Bmp4 arches (Figs 2, 3). Expression of the intermediate (joint) marker *nkx3.2* was also expanded in *UAS*:Edn1 embryos and absent in *UAS*:Bmp4 embryos (Fig. 3J-L). We next analyzed the expression of *epha4b*, as well as *msxe*, which marks a ventral subset of the broader *dlx3b*-expressing intermediate domain in wild types (Fig. 3S-U). Whereas *msxe* and *epha4b* were markedly expanded in *UAS*:Bmp4 embryos, they were only moderately so in *UAS*:Edn1 embryos (Fig. 3A-F). Furthermore, dorsal genes such as *jag1b* and *hey1* were similarly reduced in *UAS*:Bmp4 and *UAS*:Edn1 embryos (Fig. 3M-R). In contrast to

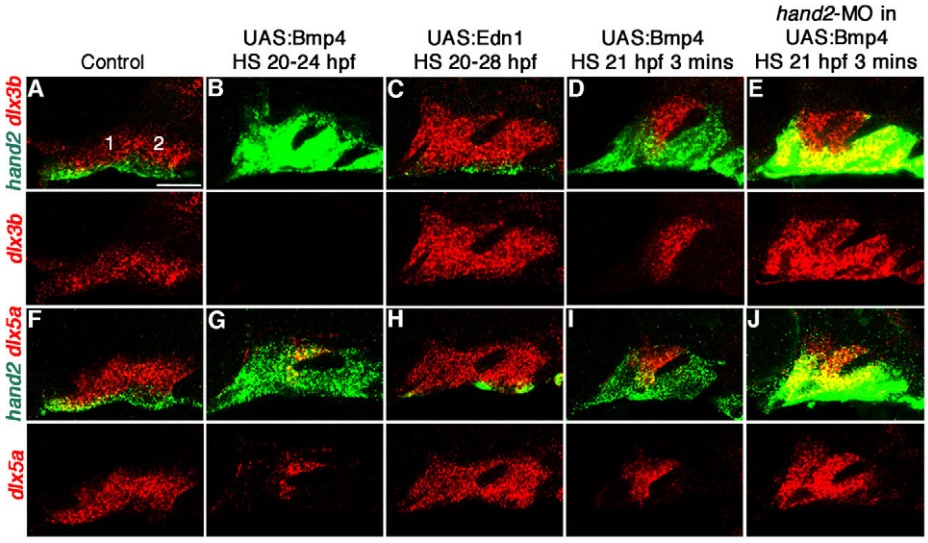

Fig. 2. Distinct effects of Bmp4 and Edn1 misexpression on *hand2* and *dlx3b/5a* expression. (**A-J**) Confocal sections of in situ hybridization for *hand2* (green) with *dlx3b* (red, A-E) or *dlx5a* (red, F-J) in the mandibular (1) and hyoid (2) arches of 36 hpf control *hsp70I*:Gal4 (A,F) and *hsp70I*:Gal4; *UAS*:Bmp4 embryos subjected to a 20-24 hpf heat-shock (B,G), as well as *hsp70I*:Gal4; *UAS*:Edn1 embryos subjected to a 20-28 hpf heat-shock (C,H). (A,F) In controls, *hand2* (*n*=48/48) was restricted to the ventral domain, and *dlx3b* (*n*=30/30) and *dlx5a* (*n*=18/18) to intermediate domains. (B,G) In *UAS*:Bmp4 embryos, *hand2* was upregulated (*n*=23/32), *dlx3b* was variably expanded (*n*=11/21) or reduced (*n*=9/21), and *dlx5a* was also variably expanded (*n*=4/20) or reduced (*n*=9/20). (C,H) In *UAS*:Edn1 embryos, *hand2* was reduced (*n*=34/34) and *dlx3b* (*n*=20/20) and *dlx5a* (*n*=14/14) were expanded. (D,E,I,J) Un-injected *hsp70I*:Gal4; *UAS*:Bmp4 embryos subjected to a 3-minute heat-shock at 21 hpf (D,I) never showed co-localization of *hand2* with *dlx3b* (*n*=0/29) or *dlx5a* (*n*=0/21), whereas *hand2* colocalized with *dlx3b* (*n*=21/35) and *dlx5a* (*n*=16/16) in *hand2*-MO-injected embryos (E,J). Anterior is towards the left and dorsal is upwards. Scale bar: 50 μm.

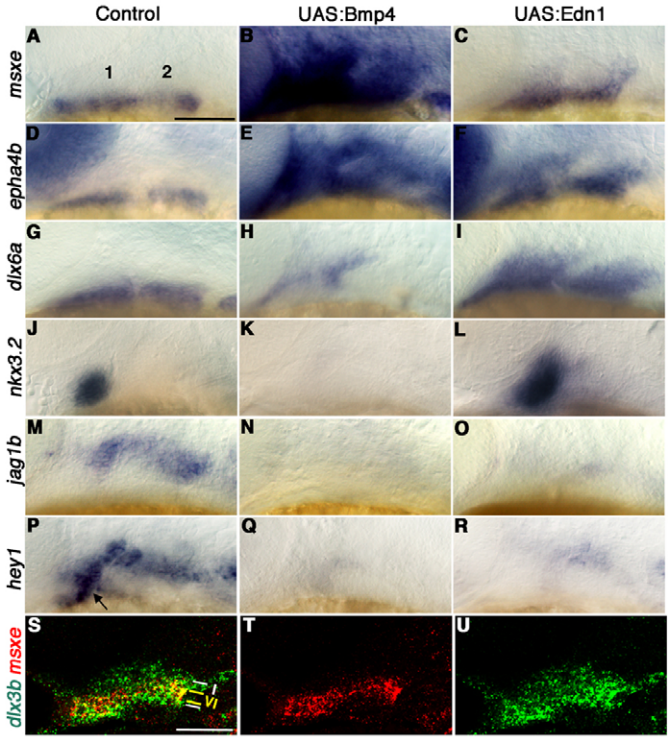

Fig. 3. DV gene expression in Bmp4 and Edn1 misexpression embryos. (A-R) In situ hybridization shows gene expression in the mandibular (1) and hyoid (2) arches of control *hsp70l*:Gal4 and *hsp70l*:Gal4; *UAS*:Bmp4 embryos subjected to a 20-24 hpf heat-shock and *hsp70l*:Gal4; *UAS*:Edn1 embryos subjected to a 20-28 hpf heat-shock. (**A-C**) *msxe* (36 hpf): compared with controls (A, *n*=22), expression was markedly expanded in *UAS*:Bmp4 (B, *n*=17/18) and slightly expanded in *UAS*:Edn1 (C, *n*=10/12) embryos. (**D-F**) *epha4b* (36 hpf): compared with controls (D, *n*=11), expression was markedly expanded in *UAS*:Bmp4 (E, *n*=12/12) and moderately expanded in *UAS*:Edn1 (F, *n*=20/20) embryos. (**G-I**) *dlx6a* (36 hpf): compared with controls (G, *n*=8), expression was variably expanded (*n*=4/7) or reduced (*n*=3/7) in *UAS*:Bmp4 (H), and markedly expanded in *UAS*:Edn1 (I, *n*=28/28) embryos. (**J-L**) *nkx3.2* (44 hpf): compared with controls (J, *n*=13), expression was lost in *UAS*:Bmp4 (K, *n*=9/9) and expanded in *UAS*:Edn1 (L, *n*=21/25) embryos. (**M-O**) *jag1b* (36 hpf): compared with controls (M, *n*=14), expression was reduced in *UAS*:Bmp4 (N, *n*=14/20) and *UAS*:Edn1 (O, *n*=21/25) embryos. (**P-R**) *hey1* (36 hpf): compared with controls (P, *n*=36), expression was reduced in *UAS*:Bmp4 (Q, *n*=26/27) and *UAS*:Edn1 (R, *n*=19/26) embryos. Arrow indicates *hey1* staining in ventral mesoderm. (**S-U**) Confocal sections of in situ hybridizations for *dlx3b* (green) and *msxe* (red) in a 36 hpf wild-type embryo. Merged (S) and single (T,U) panels are shown. Intermediate (I) and ventral-intermediate (VI) domains are depicted. Scale bars: 50 μm.

earlier stages (Alexander et al., 2011), these results suggest quite distinct roles for BMP and Edn1 signaling after 24 hpf, with BMPs strongly promoting ventral (*hand2*) and ventral-intermediate (*msxe*) gene expression and Edn1 promoting more intermediate (*dlx3b/5a/6a* and *nkx3.2*) gene expression.

Dlx expression can either expand or disappear upon Bmp4 misexpression, even within different arches of the same embryo. By 36 hpf, *hand2* expression is excluded from the intermediate *dlx3b/5a*-expressing domains of wild types (Fig. 2A,F). Similarly, in *UAS*:Bmp4 embryos heat-shocked for shorter times, the expansion of *dlx3b* and *dlx5a* expression was confined to regions lacking *hand2* expression (Fig. 2D,I). As Hand2 represses *dlx3b* and *dlx5a* in ventral CNCCs (Miller et al., 2003; Talbot et al., 2010), we tested whether the strong induction of Hand2 by Bmp4 caused the loss of intermediate gene expression seen in our gain-of-function experiments. Indeed, reduction of Hand2 function with a *hand2*-MO (Maves et al., 2009) resulted in expansion of *dlx3b* and *dlx5a* expression throughout the arches of *UAS*:Bmp4 embryos (Fig. 2E,J). Hence, Bmp4 acts in a dose-dependent manner during DV facial patterning, with lower BMP promoting intermediate gene expression and higher BMP promoting Hand2, which subsequently inhibits expression of intermediate Dlx genes.

Cell-autonomous requirements for BMP signaling in CNCCs

Whereas reduction of BMP signaling in *Tg*(*hsp70l:dnBmpr1a-GFP*) embryos results in loss of *hand2*, *msxe* and *dlx3b* expression, BMP signaling also regulates *edn1* expression in the ventral ectoderm (Alexander et al., 2011). To discriminate cell-autonomous roles of BMP signaling from indirect roles such as *edn1* regulation, we transplanted wild-type *Tg*(*fli1a:GFP*) or *Tg*(*hsp70l:dnBmpr1a-GFP*) CNCC precursors into wild types and examined gene expression in the GFP$^+$ donor cells. Whereas wild-type *fli1a*:GFP$^+$ donor CNCCs showed normal *dlx3b* (*n*=5), *msxe* (*n*=3) and *hand2* (*n*=5) expression when compared with unlabeled host CNCCs, *hsp70l:*dnBmpr1a-GFP$^+$ donor CNCCs showed a cell-autonomous lack of *hand2* (*n*=5/5) and *msxe* (*n*=6/6) expression yet no change in *dlx3b* (*n*=0/6) expression (Fig. 4). Thus, our mosaic analyses indicate that BMP signaling acts cell-autonomously in CNCCs for ventral (*hand2* and *msxe*) but not intermediate (*dlx3b*) gene expression.

Bmp4 can induce *hand2* and *msxe* independently of Edn1

The cell-autonomous requirement for BMP responsiveness in *hand2* and *msxe* expression suggests that BMPs promote expression directly, rather than through induction of ectodermal *edn1* expression. To further investigate this model, we analyzed whether ectopic Bmp4 can induce DV gene expression in the genetic absence of Edn1. As previously reported (Miller et al., 2000), *edn1*$^{-/-}$ mutants have a near complete loss of *hand2*, *dlx3b* and *msxe* expression at 36 hpf (Fig. 5E,M). Consistent with Bmp4 misexpression rescuing the ventral but not intermediate skeletal defects of *edn1*$^{-/-}$ mutants (Alexander et al., 2011), we found that Bmp4 induced *hand2* and *msxe*, but not *dlx3b*, in arch CNCCs in a dose-dependent manner in *edn1*$^{-/-}$; *UAS*:Bmp4 embryos (Fig. 5). However, *hand2* and *msxe* induction required higher doses of Bmp4 in *edn1*$^{-/-}$ mutants compared with wild-type siblings, indicating that Edn1 is required for maximal induction of these genes by Bmp4. In addition, injection of *hand2*-MO into *edn1*$^{-/-}$; *UAS*:Bmp4 embryos did not restore *dlx3b* expression (supplementary material Fig. S3), suggesting that the failure of Bmp4 to induce *dlx3b* expression in *edn1*$^{-/-}$ mutants is not due to Hand2 repression. We therefore conclude that BMPs can activate *hand2* and *msxe* expression independently of Edn1, yet require Edn1 for regulation of *dlx3b* expression.

Edn1 and Jag1b promote Grem2 expression in dorsal and intermediate CNCCs

As BMPs strongly promote *hand2* expression, yet normally only do so in the ventral-most regions of the arches, we investigated whether BMP antagonists restrict BMP signaling ventrally. Grem2 was a good candidate as it is expressed in the arches during these

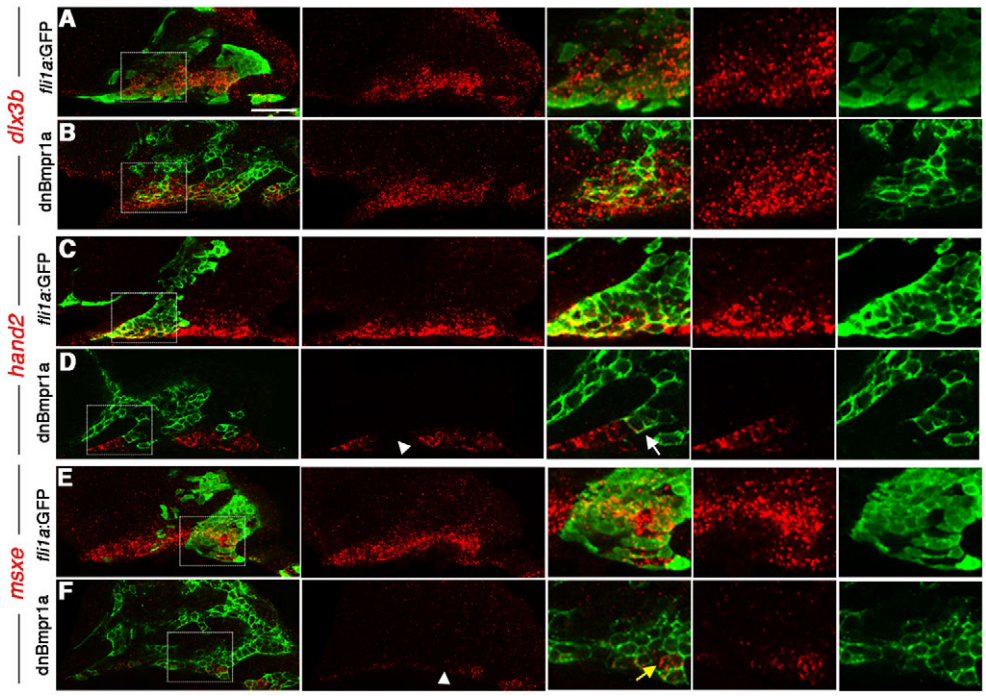

Fig. 4. Cell-autonomous regulation of DV gene expression by BMP. (**A-F**) Confocal sections of anti-GFP staining (green) and *dlx3b* (A,B), *hand2* (C,D) and *msxe* (E,F) expression (red). Merged and individual channels are shown, as well as higher magnification views of boxed regions. Wild-type hosts received CNCC precursor transplants from either wild-type *fli1a*:GFP (A,C,E) or *hsp70l*:dnBmpr1a-GFP (B,D,F) donors. *hand2* and *msxe* were cell-autonomously reduced in *hsp70l*:dnBmpr1a-GFP clones (white arrowheads), whereas *dlx3b* was largely unaffected. In high magnification views, the white arrow indicates a *hsp70l*:dnBmpr1a-GFP clone displaying loss of *hand2*, and the yellow arrow indicates a small clone of wild-type host cells still expressing *msxe*. Scale bar: 50 μm.

early stages of DV patterning (Müller et al., 2006). Using double fluorescent in situ hybridization with the CNCC marker *dlx2a*, we found that *grem2* was expressed in dorsal and intermediate CNCCs of the arches (Fig. 6A; supplementary material Fig. S4A). The *grem2* expression domain partially overlaps with intermediate *dlx3b* and dorsal *jag1b* expression, and most strongly overlaps with expression of the Jag1b-Notch2 target gene *hey1* (supplementary material Fig. S4). Consistently, we found that *grem2* expression was substantially reduced in *jag1b*^{b1105} mutants (Fig. 6B). *grem2* expression was also reduced in *edn1*$^{-/-}$ mutants and expanded in *UAS*:Edn1 embryos (Fig. 6C,D). This induction by Edn1 is required to suppress BMP signaling in intermediate and dorsal domains, as arch expression from a *BRE*:GFP transgenic line (Alexander et al., 2011) expanded in *edn1*$^{-/-}$ mutants (Fig. 6G,H). By contrast, BMPs inhibit *grem2* as expression was shifted ventrally in *hsp70l*:dnBmpr1a-GFP embryos and lost in *UAS*:Bmp4 embryos (Fig. 6E,F). Hence, a combination of Jag1b and Edn1 activation and BMP inhibition restricts *grem2* expression to dorsal-intermediate CNCCs.

Grem2 is required for dorsal and intermediate skeletal patterning

To investigate whether Grem2 is required to restrict BMP activity to ventral CNCCs, we designed two independent translation-blocking MOs against *grem2*. Of the two MOs, *grem2*-MO #1 was used for further analysis as it most effectively blocked translation from a Grem2:GFP fusion construct containing the MO-recognition site (Fig. 7A-C). Injection of *grem2*-MO into *BRE*:GFP fish increased BMP activity in the dorsal and intermediate arches at 36 hpf (Fig. 7D,E). In addition, *grem2*-MO caused dorsal and intermediate skeletal defects similar to those seen with moderate increases in BMP signaling (Fig. 7J; supplementary material Fig. S5). Skeletal transformations were most apparent in the hyoid arch, with the dorsal Hm adopting a rod-shaped morphology and the Op bone acquiring a finger-like appearance (*n*=21/36; supplementary material Fig. S5B), and less frequently Hm and the intermediate Sy and joints were lost (*n*=14/36; supplementary material Fig. S5C). Consistent with these dorsal and intermediate skeletal defects, the expression of *dlx3b*, and to a lesser extent *hand2*, was moderately expanded in 36 hpf *grem2*-MO-injected embryos (Fig. 7G). As with moderate Bmp4 misexpression (Alexander et al., 2011), reducing Grem2 function rescued development of the ventral (M and Ch) but not the intermediate (Sy and joints) skeleton in 15/24 *edn1*$^{-/-}$ mutants (Fig. 7M). These effects were specific because: (1) co-injection of *grem2*-MO #1 and #2 at sub-threshold doses caused highly penetrant synergistic effects on dorsal skeletal development; (2) *grem2*-MO #2 also restored the ventral facial skeleton in 6/12 *edn1*$^{-/-}$ mutants; and (3) arch misexpression of Grem2 (see details below) partially rescued the dorsal skeletal defects of *grem2*-MO-injected embryos (supplementary material Fig. S5). These data strongly indicate that Grem2 is required for patterning of the dorsal and intermediate facial skeleton.

Grem2 misexpression dorsalizes the ventral facial skeleton

In order to test Grem2 sufficiency in dorsal skeletal patterning, we misexpressed it in the arches by subjecting *Tg*(*hsp70l:Gal4; UAS:Grem2*) embryos to a 16-17 hpf heat shock (referred to as *UAS:Grem2*). Similar to the skeletal defects of *edn1*$^{-/-}$ mutants (Fig. 7L) and *hsp70l*:dnBmpr1a-GFP embryos (Alexander et al., 2011), Grem2 misexpression caused specific defects in the ventral and intermediate skeletons. In particular, the ventral (M and Ch) and intermediate (Pq and Sy) cartilages were variably reduced and altered in shape, and the intermediate-domain-derived joints were lost in 56/72 *UAS*:Grem2 larvae (Fig. 7K; supplementary material Fig. S5G,H). Consistent with Grem2 inhibiting ventral and intermediate skeletal development, ventral *hand2* and intermediate *dlx3b* expression were almost completely lost in *UAS*:Grem2 embryos (Fig. 7H), again resembling *hsp70l*:dnBmpr1a-GFP (Alexander et al., 2011) and *edn1*$^{-/-}$ (Fig. 5E) embryos. We

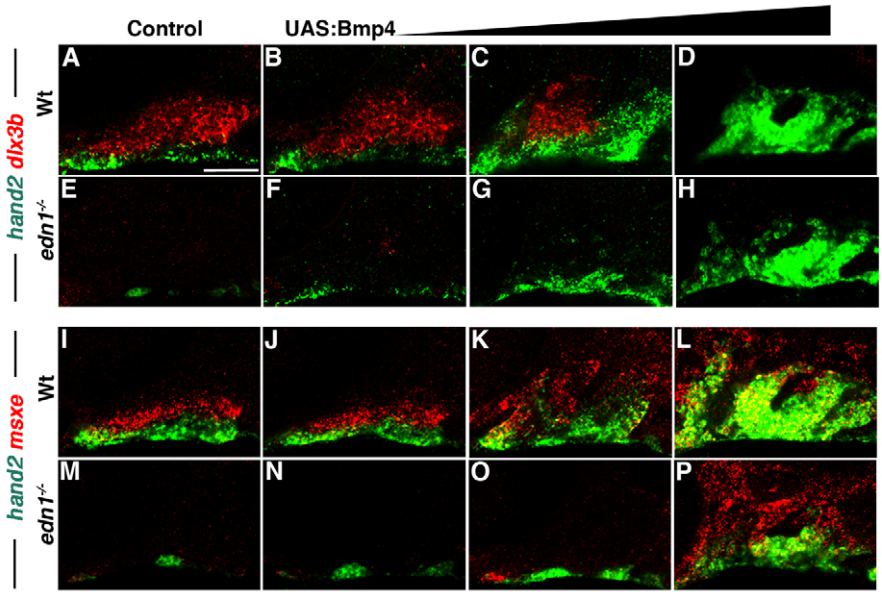

Fig. 5. Bmp4 induces *hand2* and *msxe* expression in the absence of Edn1. (**A-P**) Confocal sections of 36 hpf in situ hybridizations for *hand2* (green) with *dlx3b* (red, A-H) or *msxe* (red, I-P) in control *hsp70l*:Gal4 (A,I), *edn1*$^{-/-}$ mutant (E,M), *UAS*:Bmp4 (B-D,J-L) and *edn1*$^{-/-}$; *UAS*:Bmp4 (F-H,N-P) embryos. Increasing periods of Bmp4 heat-shock induction [1 minute at 21 hpf (B,F,J,N), 3 minutes at 21 hpf (C,G,K,O) and 4 hours from 20-24 hpf (D,H,L,P)] resulted in progressive recovery of *hand2* and *msxe* but not *dlx3b* expression in *edn1*$^{-/-}$ mutants. Consistent phenotypes were observed for the following: (A) *n*=55, (B) *n*=31, (C) *n*=15, (D) *n*=9, (E) *n*=8, (F) *n*=3, (G) *n*=4, (H) *n*=1, (I) *n*=37, (J) *n*=11, (K) *n*=6, (L) *n*=9, (M) *n*=20, (N) *n*=2, (O) *n*=3 and (P) *n*=2. Scale bar: 50 μm.

therefore conclude that the ventral exclusion of *grem2* expression is crucial for development of the ventral and intermediate facial skeleton.

DISCUSSION

Here, we show that BMP and Edn1 signaling play distinct roles in specifying ventral and intermediate domains, respectively, of the pharyngeal arches. Whereas misexpression of Bmp4 or Edn1 can partially compensate for the loss of the other at early stages, we find that BMP activity later becomes restricted and plays a more prominent role in development of the ventral-most facial skeleton. This restriction of BMP activity to the ventral face is accomplished in part by Edn1- and Jag1b-mediated induction of the BMP antagonist Grem2 in the intermediate and dorsal face. Together, these results support a model of DV facial patterning in which cross-inhibitory interactions between initially redundant BMP and Edn1 signaling pathways result in the segregation of facial skeletal precursors into distinct ventral and intermediate domains.

BMPs and Edn1 have distinct roles in DV patterning of the face

Whereas Edn1 and BMP signaling are both required for ventral and intermediate facial skeletal development (Alexander et al., 2011), our gain-of-function studies reveal that misexpression of Bmp4 but not Edn1 disrupts the development of the intermediate skeleton, including the joints. Such a result is consistent with BMPs having a distinct role in promoting ventral at the expense of intermediate skeletal fates. These different roles of BMPs and Edn1 in ventral versus intermediate facial patterning are also reflected in the earlier regulation of DV gene expression. Whereas Bmp4 misexpression strongly induces the ventral genes *hand2* and *msxe*, Edn1 more prominently induces intermediate genes such as *dlx3b*/*dlx5a*/*dlx6a* and *nkx3.2*. Previous studies have shown that as arch development progresses, *hand2* becomes restricted to a distinct ventral domain from the more intermediate expression of *dlx3b/5a/6a* and *nkx3.2* (Miller et al., 2003; Talbot et al., 2010). Moreover, we show here that DV gene expression is further refined, with *msxe* expression

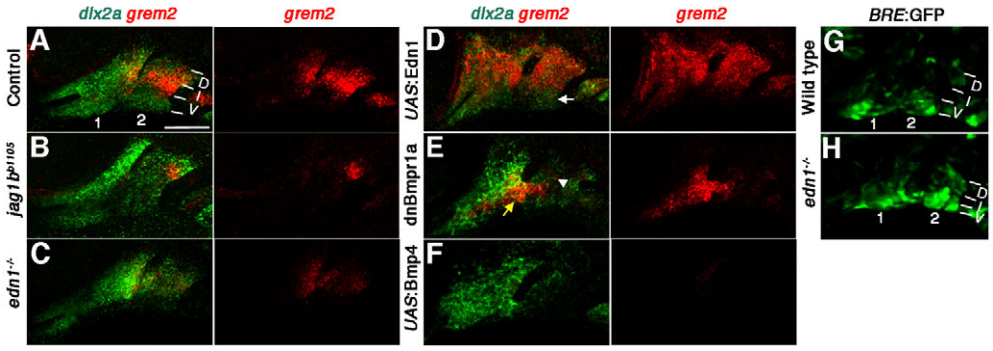

Fig. 6. Edn1 and Jag1b negatively regulate *grem2* expression. (**A-F**) Confocal sections of in situ hybridization for *grem2* (red) and *dlx2a* (green) in controls (A, *n*=62), *jag1b*^{b1105} mutant (B, *n*=9), *edn1*$^{-/-}$ mutant (C, *n*=5), *UAS*:Edn1 (D, *n*=17), *hsp70l*:dnBmpr1a-GFP (E, *n*=32) and *UAS*:Bmp4 (F, *n*=23) embryos at 36 hpf. In *UAS*:Edn1 embryos, *grem2* expression was seen throughout the mandibular and hyoid arches, except for the ventral-most domain (white arrow). In *hsp70l*:dnBmpr1a-GFP embryos, *grem2* expression shifted to ventral regions (yellow arrow) and was reduced dorsally (white arrowhead). Dorsal (D), intermediate (I) and ventral (V) domains of the mandibular (1) and hyoid (2) arches are labeled. Scale bar: 50 μm. (**G**,**H**) *BRE*:GFP expression increased throughout the dorsal and intermediate arch domains of *edn1*$^{-/-}$ mutants (*n*=4) compared with wild-type siblings (*n*=16).

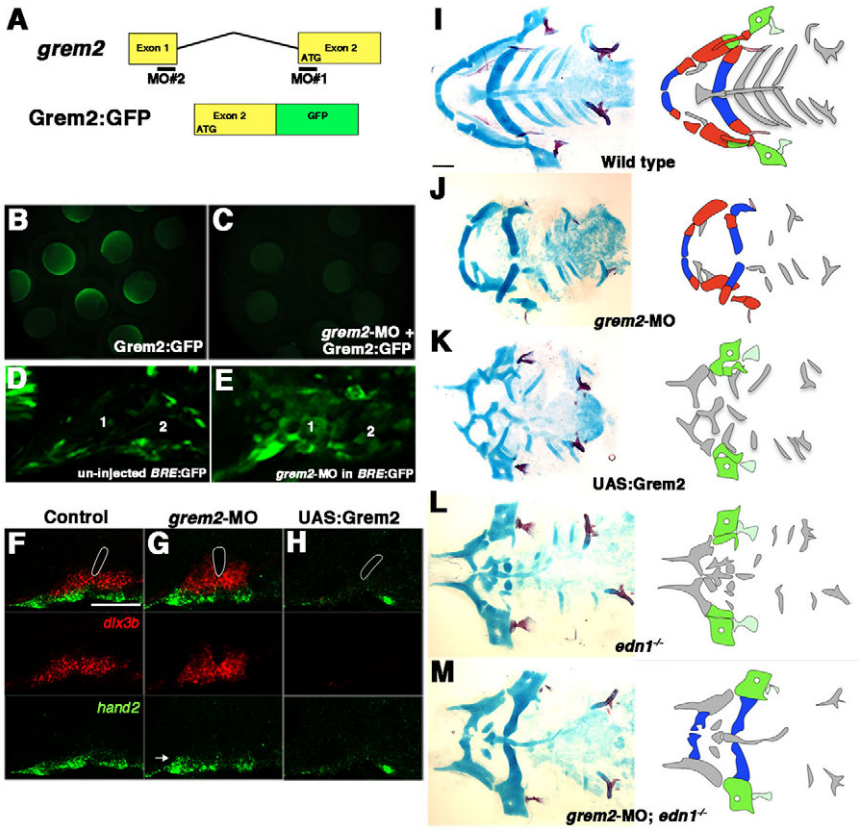

Fig. 7. Grem2 promotes the dorsal and intermediate facial skeleton. (**A**) Structure of the *grem2* gene and the Grem2:GFP fusion construct. *grem2*-MO #1 recognizes the ATG start site in Exon 2 and grem2-MO #2 recognizes the 5′ UTR. (**B**,**C**) Grem2:GFP fluorescence in uninjected (B) or *grem2*-MO-#1-injected (C) embryos at 9 hpf. (**D**,**E**) Confocal sections of 30 hpf *BRE*:GFP transgenic embryos. Compared with uninjected controls (D, *n*=5), injection of *grem2*-MO-#1 (E, *n*=8) increased *BRE*:GFP throughout the mandibular (1) and hyoid (2) arches. (**F-H**) Confocal sections of in situ hybridizations for *hand2* (green) and *dlx3b* (red). Relative to the first pouch (white outlines), *dlx3b* and *hand2* were mildly expanded in *grem2*-MO embryos (G, *n*=45/52) and lost in *hsp70l*:Gal4; *UAS*:Grem2 embryos subjected to a 16-17 hpf heat-shock (H, *n*=16/16). Arrow indicates expanded *hand2* expression. (**I-M**) Ventral views of 5 dpf facial skeletons from control (I), *grem2*-MO-#1-injected (J), *UAS*:Grem2 (K), *edn1*$^{-/-}$ mutant (L) and an *edn1*$^{-/-}$ mutant injected with *grem2*-MO-#1 (M). Schematics show skeletal regions derived from dorsal (green), intermediate (red) and ventral (blue) arch domains, with bones lightly shaded. Elements of undefined morphology or derived from the maxillary domain or more posterior arches are grey. Scale bar: 50 μm.

marking a ventral-intermediate domain within the broader *dlx3b*-positive intermediate domain. Hence, BMPs may serve to segregate ventral *hand2*$^{+}$/*msxe*$^{-}$/*dlx3b*$^{-}$ and ventral-intermediate *hand2*$^{-}$/*msxe*$^{+}$/*dlx3b*$^{+}$ skeletal precursors from more intermediate *hand2*$^{-}$/*msxe*$^{-}$/*dlx3b*$^{+}$ precursors (Fig. 8).

Our findings in zebrafish also agree with those in avians and mice showing that Msx1, Msx2 and Hand2 are regulated by BMP signaling (Tucker et al., 1998; Liu et al., 2004; Liu et al., 2005; Mariani et al., 2008), whereas Dlx3, Dlx5 and Dlx6 (but not Hand2) are strongly induced by Edn1 (Sato et al., 2008). Although BMPs promote *edn1* expression in the ectoderm (Alexander et al., 2011), two lines of evidence argue that BMP signaling also regulates *hand2* and *msxe* expression more directly: (1) Bmp4 can induce the expression of *hand2* and *msxe*, but not *dlx3b*, in the genetic absence of Edn1; and (2) BMP responses are required cell-autonomously in CNCCs for the expression of *hand2* and *msxe* but not *dlx3b*. We therefore conclude that BMP signaling probably functions directly to regulate Hand and Msx gene expression in the ventral arches, but may function indirectly through Edn1 to regulate Dlx family expression in intermediate domains. Conversely, the more prominent role of Edn1 in intermediate skeletal development would explain why the intermediate skeleton is particularly sensitive to partial reductions of Edn1 signaling (Miller and Kimmel, 2001; Walker et al., 2006).

An important consideration is that the roles of BMPs and Edn1 may change as arch development progresses. DV gene expression is highly dynamic within the developing pharyngeal arches, with Hand2 and Dlx family gene expression colocalizing in the early ventral arches and later becoming segregated into distinct ventral and intermediate domains (Talbot et al., 2010; Barron et al., 2011). Dlx5 and Dlx6 are required for the initial arch expression of *Hand2* in mice (Depew et al., 2002; Ruest et al., 2004), and we find that BMPs and Edn1 have overlapping roles in early *dlx5a/6a* expression (Alexander et al., 2011). However, once Hand2 reaches a specific level it begins to inhibit Dlx family and Nkx3.2 gene expression in the ventral arches (Miller et al., 2003; Talbot et al., 2010; Barron et al., 2011). Thus, as arch development progresses, arch elongation and the expression of Grem2 in dorsal-intermediate domains would progressively restrict BMP activity and hence Hand2 to the ventral-most arches, where it would inhibit Dlx family and Nkx3.2 expression. In this model, the lack of Hand2 in the intermediate domain presumably allows continued Dlx family and Nkx3.2 expression (Fig. 8B).

Edn1 and Jag1b function through Grem2 to restrict BMP activity to the ventral face

Our genetic data indicate that the later restriction of BMP activity to the ventral arches is crucial for proper development of intermediate and dorsal skeletal precursors. Whereas previous studies in mice have shown roles for the BMP antagonists Noggin and Chordin in restricting BMP activity during mandibular development, *Noggin* is expressed in ventral arch epithelium and *Chordin* weakly throughout the arches (Stottmann et al., 2001). By contrast, we show here that zebrafish *grem2* is expressed in a dorsal-intermediate arch domain that opposes ventral *bmp4* expression. Consistent with Grem2 restricting BMP signaling to the ventral domain, reduction of Grem2 results in upregulated BMP activity and altered skeletal development in the dorsal and intermediate face.

As Edn1 is a potent inducer of *grem2*, Edn1 may pattern the intermediate domain in part by keeping BMP activity below the threshold required for *hand2* expression, thus preventing Hand2 repression of *dlx3b/5a/6a* and *nkx3.2* expression. In the dorsal domain, Jag1b would further contribute to *grem2* induction and

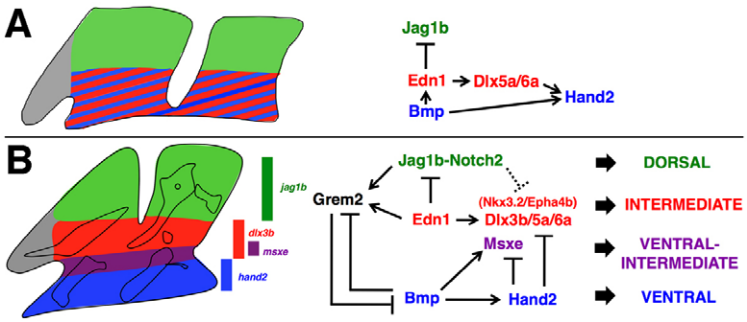

Fig. 8. Model of DV arch patterning. (**A**) In the early arches (24 hpf), Hand2 and Dlx family genes are co-expressed ventrally. BMPs both directly, and indirectly via Edn1 and Dlx5/6, initiate *hand2* expression ventrally. (**B**) In the later arches (36 hpf), higher BMP activity induces *hand2* and *msxe* in ventral and ventral-intermediate domains, respectively, with Hand2 repressing intermediate genes such as *dlx3b/5a/6a* and *nkx3.2*. In the intermediate domain, Edn1 induces *dlx3b/5a/6a* and *nkx3.2*, and represses *jag1b*. In addition, Edn1 and Jag1b together induce *grem2*, with Grem2 inhibition of BMP signaling preventing Hand2-dependent inhibition of intermediate genes. In the dorsal domain, Jag1b-Notch2 signaling may repress intermediate genes directly (dotted line) and/or indirectly through Grem2-mediated inhibition of BMP signaling.

BMP inhibition. A role for Jag1b in Grem2 induction would explain why loss of Jag1b rescues ventral skeletal defects in *edn1*$^{-/-}$ mutants (Zuniga et al., 2010), similar to depleting Grem2 (this paper) or misexpressing Bmp4 (Alexander et al., 2011). In *edn1*$^{-/-}$ mutants, a reduction of *grem2* expression correlates with increased BMP activity, yet this is not sufficient to support ventral development in the absence of Edn1. Significantly, some residual *grem2* expression remains in *edn1*$^{-/-}$ mutants, probably owing to Jag1b regulation. One possibility then is that depletion of remaining *grem2* would increase BMP signaling above a threshold required to induce *hand2* and *msxe* expression independently of Edn1, thus rescuing the ventral skeleton. However, we were unable to detect further increases in *BRE*:GFP expression upon depletion of *grem2* in *edn1*$^{-/-}$ mutants (data not shown), suggesting that only a minor further increase in BMP activity is needed to rescue loss of Edn1, consistent with the very short *UAS*:Bmp4 heat shocks required to rescue *edn1*$^{-/-}$ mutants (Alexander et al., 2011). Moreover, as we find that BMP4 inhibits *jag1b* expression, BMPs might also function upstream of Jag1b to prevent Jag1b-mediated repression of ventral fates. An analogous Jag1-Gremlin-Bmp4 module has been described in the limb, with Gremlin1 inhibition of Bmp4 promoting Jag1 expression in the distal limb bud mesenchyme (Panman et al., 2006).

Based on our findings, we propose a network model of craniofacial patterning in which positive and negative feedback progressively creates two states of BMP signaling: high BMP activity in the ventral domain; and low BMP in the intermediate and dorsal domains. In the ventral domain, BMP-mediated repression of its own inhibitor, Grem2, reinforces BMP signaling. In the intermediate and dorsal domains, combined Edn1 and Jagged-Notch signaling induces Grem2 and inhibits BMP signaling, with reduced BMP-mediated repression of Grem2 reinforcing the low BMP state. Indeed, visualization of BMP activity by either *BRE*:GFP or phospho-SMAD staining suggests a two-state model as opposed to a gradient of BMP responses (Alexander et al., 2011). One property of this feedback model of DV patterning is that it creates a sharp boundary between two domains, with BMP signaling self-reinforcing to either high or low levels depending on the initial activity relative to a specific threshold. Such a self-reinforcing BMP network would create robustness. For example, the underlying ventral bias of BMP signaling would explain why the unlocalized injection of Edn1 protein throughout the arches can largely restore normal DV patterning to zebrafish *edn1*$^{-/-}$ mutants (Miller et al., 2000), a result not predicted if Edn1 functioned in isolation as a morphogen.

If both Bmp4 and Edn1 are secreted from the ventral ectoderm, an important question is why BMP responses become restricted ventrally, whereas Edn1 responses become more restricted to intermediate domains. In one model, arch CNCCs are exposed to different ratios of Bmp4 and Edn1, with the former higher ventrally. Distinct diffusion coefficients or the unique expression domains of these ligands might explain such differences. Indeed, we observe that *bmp4* is expressed in a more ventral domain of facial ectoderm than *edn1*. Alternatively, the added input of Jagged-Notch signaling on *grem2* expression might increase total Grem2 levels beyond what can be inhibited by BMP, thus reducing BMP activity to below a threshold required to maintain itself in dorsal and intermediate CNCCs. Future modeling studies will be needed to understand how BMP, Edn1 and Jagged-Notch signaling are integrated to generate such highly reproducible pre-skeletal domains within the developing face.

Acknowledgements
We thank Megan Matsutani, Corey Gingerich, Tailin Zhang and Ines Gehring for fish care, Miriam Lassiter and Ankita Das for *UAS*:Grem2 fish, and Geoff and Caroline Burns for the pDestTol2AB2 construct.

Funding
Research was supported by the National Institutes of Health [F31DE020248 to E.Z., R01DE018405 and R01DE018405-S03 to J.G.C., and R01DE13828 to T.F.S.]; and March of Dimes [FY08-459 to J.G.C.]. Deposited in PMC for release after 12 months.

Competing interests statement
The authors declare no competing financial interests.

Supplementary material
Supplementary material available online at
http://dev.biologists.org/lookup/suppl/doi:10.1242/dev.067785/-/DC1

References
Alexander, C., Zuniga, E., Blitz, I. L., Wada, N., Le Pabic, P., Javidan, Y., Zhang, T., Cho, K. W., Crump, J. G. and Schilling, T. F. (2011). Combinatorial roles for BMPs and Endothelin 1 in patterning the dorsal-ventral axis of the craniofacial skeleton. *Development* **138**, 5135-5146.
Bardot, B., Lecoin, L., Huillard, E., Calothy, G. and Marx, M. (2001). Expression pattern of the drm/gremlin gene during chicken embryonic development. *Mech. Dev.* **101**, 263-265.
Barron, F., Woods, C., Kuhn, K., Bishop, J., Howard, M. J. and Clouthier, D. E. (2011). Downregulation of Dlx5 and Dlx6 expression by Hand2 is essential for initiation of tongue morphogenesis. *Development* **138**, 2249-2259.
Beverdam, A., Merlo, G. R., Paleari, L., Mantero, S., Genova, F., Barbieri, O., Janvier, P. and Levi, G. (2002). Jaw transformation with gain of symmetry after Dlx5/Dlx6 inactivation: mirror of the past? *Genesis* **34**, 221-227.
Charite, J., McFadden, D. G., Merlo, G., Levi, G., Clouthier, D. E., Yanagisawa, M., Richardson, J. A. and Olson, E. N. (2001). Role of Dlx6 in regulation of an endothelin-1-dependent, dHAND branchial arch enhancer. *Genes Dev.* **15**, 3039-3049.
Crump, J. G., Swartz, M. E. and Kimmel, C. B. (2004). An integrin-dependent role of pouch endoderm in hyoid cartilage development. *PLoS Biol.* **2**, E244.
Crump, J. G., Swartz, M. E., Eberhart, J. K. and Kimmel, C. B. (2006). Moz-dependent Hox expression controls segment-specific fate maps of skeletal precursors in the face. *Development* **133**, 2661-2669.
Depew, M. J., Lufkin, T. and Rubenstein, J. L. (2002). Specification of jaw subdivisions by Dlx genes. *Science* **298**, 381-385.

Eberhart, J. K., Swartz, M. E., Crump, J. G. and Kimmel, C. B. (2006). Early Hedgehog signaling from neural to oral epithelium organizes anterior craniofacial development. *Development* **133**, 1069-1077.
Francis-West, P. H., Tatla, T. and Brickell, P. M. (1994). Expression patterns of the bone morphogenetic protein genes Bmp-4 and Bmp-2 in the developing chick face suggest a role in outgrowth of the primordia. *Dev. Dyn.* **201**, 168-178.
Graham, A., Francis-West, P., Brickell, P. and Lumsden, A. (1994). The signalling molecule BMP4 mediates apoptosis in the rhombencephalic neural crest. *Nature* **372**, 684-686.
Holzschuh, J., Wada, N., Wada, C., Schaffer, A., Javidan, Y., Tallafuss, A., Bally-Cuif, L. and Schilling, T. F. (2005). Requirements for endoderm and BMP signaling in sensory neurogenesis in zebrafish. *Development* **132**, 3731-3742.
Hsu, D. R., Economides, A. N., Wang, X., Eimon, P. M. and Harland, R. M. (1998). The Xenopus dorsalizing factor Gremlin identifies a novel family of secreted proteins that antagonize BMP activities. *Mol. Cell* **1**, 673-683.
Kanzler, B., Foreman, R. K., Labosky, P. A. and Mallo, M. (2000). BMP signaling is essential for development of skeletogenic and neurogenic cranial neural crest. *Development* **127**, 1095-1104.
Kimmel, C. B., Ballard, W. W., Kimmel, S. R., Ullmann, B. and Schilling, T. F. (1995). Stages of embryonic development of the zebrafish. *Dev. Dyn.* **203**, 253-310.
Kimmel, C. B., Walker, M. B. and Miller, C. T. (2007). Morphing the hyomandibular skeleton in development and evolution. *J. Exp. Zool. B Mol. Dev. Evol.* **308**, 609-624.
Kurihara, Y., Kurihara, H., Suzuki, H., Kodama, T., Maemura, K., Nagai, R., Oda, H., Kuwaki, T., Cao, W. H., Kamada, N. et al. (1994). Elevated blood pressure and craniofacial abnormalities in mice deficient in endothelin-1. *Nature* **368**, 703-710.
Kwan, K. M., Fujimoto, E., Grabher, C., Mangum, B. D., Hardy, M. E., Campbell, D. S., Parant, J. M., Yost, H. J., Kanki, J. P. and Chien, C. B. (2007). The Tol2kit: a multisite gateway-based construction kit for Tol2 transposon transgenesis constructs. *Dev. Dyn.* **236**, 3088-3099.
Liem, K. F., Jr, Tremml, G., Roelink, H. and Jessell, T. M. (1995). Dorsal differentiation of neural plate cells induced by BMP-mediated signals from epidermal ectoderm. *Cell* **82**, 969-979.
Liu, W., Selever, J., Wang, D., Lu, M. F., Moses, K. A., Schwartz, R. J. and Martin, J. F. (2004). Bmp4 signaling is required for outflow-tract septation and branchial-arch artery remodeling. *Proc. Natl. Acad. Sci. USA* **101**, 4489-4494.
Liu, W., Selever, J., Murali, D., Sun, X., Brugger, S. M., Ma, L., Schwartz, R. J., Maxson, R., Furuta, Y. and Martin, J. F. (2005). Threshold-specific requirements for Bmp4 in mandibular development. *Dev. Biol.* **283**, 282-293.
Mariani, F. V., Ahn, C. P. and Martin, G. R. (2008). Genetic evidence that FGFs have an instructive role in limb proximal-distal patterning. *Nature* **453**, 401-405.
Maves, L., Tyler, A., Moens, C. B. and Tapscott, S. J. (2009). Pbx acts with Hand2 in early myocardial differentiation. *Dev. Biol.* **333**, 409-418.
Miller, C. T. and Kimmel, C. B. (2001). Morpholino phenocopies of endothelin 1 (sucker) and other anterior arch class mutations. *Genesis* **30**, 186-187.
Miller, C. T., Schilling, T. F., Lee, K., Parker, J. and Kimmel, C. B. (2000). sucker encodes a zebrafish Endothelin-1 required for ventral pharyngeal arch development. *Development* **127**, 3815-3828.
Miller, C. T., Yelon, D., Stainier, D. Y. and Kimmel, C. B. (2003). Two endothelin 1 effectors, hand2 and bapx1, pattern ventral pharyngeal cartilage and the jaw joint. *Development* **130**, 1353-1365.
Mina, M., Wang, Y. H., Ivanisevic, A. M., Upholt, W. B. and Rodgers, B. (2002). Region- and stage-specific effects of FGFs and BMPs in chick mandibular morphogenesis. *Dev. Dyn.* **223**, 333-352.
Müller, I. I., Knapik, E. W. and Hatzopoulos, A. K. (2006). Expression of the protein related to Dan and Cerberus gene – prdc – during eye, pharyngeal arch, somite, and swim bladder development in zebrafish. *Dev. Dyn.* **235**, 2881-2888.
Nair, S., Li, W., Cornell, R. and Schilling, T. F. (2007). Requirements for Endothelin type-A receptors and Endothelin-1 signaling in the facial ectoderm for the patterning of skeletogenic neural crest cells in zebrafish. *Development* **134**, 335-345.
Nguyen, V. H., Schmid, B., Trout, J., Connors, S. A., Ekker, M. and Mullins, M. C. (1998). Ventral and lateral regions of the zebrafish gastrula, including the neural crest progenitors, are established by a bmp2b/swirl pathway of genes. *Dev. Biol.* **199**, 93-110.
Nie, X., Luukko, K. and Kettunen, P. (2006). BMP signalling in craniofacial development. *Int. J. Dev. Biol.* **50**, 511-521.
Ozeki, H., Kurihara, Y., Tonami, K., Watatani, S. and Kurihara, H. (2004). Endothelin-1 regulates the dorsoventral branchial arch patterning in mice. *Mech. Dev.* **121**, 387-395.
Panman, L., Galli, A., Lagarde, N., Michos, O., Soete, G., Zuniga, A. and Zeller, R. (2006). Differential regulation of gene expression in the digit forming area of the mouse limb bud by SHH and gremlin 1/FGF-mediated epithelial-mesenchymal signalling. *Development* **133**, 3419-3428.
Platt, J. B. (1893). Ectodermic origin of the cartilages of the head. *Anat. Anz.* **8**, 506-509.
Pyati, U. J., Webb, A. E. and Kimelman, D. (2005). Transgenic zebrafish reveal stage-specific roles for Bmp signaling in ventral and posterior mesoderm development. *Development* **132**, 2333-2343.
Ruest, L. B., Xiang, X., Lim, K. C., Levi, G. and Clouthier, D. E. (2004). Endothelin-A receptor-dependent and -independent signaling pathways in establishing mandibular identity. *Development* **131**, 4413-4423.
Sato, T., Kurihara, Y., Asai, R., Kawamura, Y., Tonami, K., Uchijima, Y., Heude, E., Ekker, M., Levi, G. and Kurihara, H. (2008). An endothelin-1 switch specifies maxillomandibular identity. *Proc. Natl. Acad. Sci. USA* **105**, 18806-18811.
Scheer, N. and Campos-Ortega, J. A. (1999). Use of the Gal4-UAS technique for targeted gene expression in the zebrafish. *Mech. Dev.* **80**, 153-158.
Shigetani, Y., Nobusada, Y. and Kuratani, S. (2000). Ectodermally derived FGF8 defines the maxillomandibular region in the early chick embryo: epithelial-mesenchymal interactions in the specification of the craniofacial ectomesenchyme. *Dev. Biol.* **228**, 73-85.
Steventon, B., Araya, C., Linker, C., Kuriyama, S. and Mayor, R. (2009). Differential requirements of BMP and Wnt signalling during gastrulation and neurulation define two steps in neural crest induction. *Development* **136**, 771-779.
Stottmann, R. W., Anderson, R. M. and Klingensmith, J. (2001). The BMP antagonists Chordin and Noggin have essential but redundant roles in mouse mandibular outgrowth. *Dev. Biol.* **240**, 457-473.
Talbot, J. C., Johnson, S. L. and Kimmel, C. B. (2010). hand2 and Dlx genes specify dorsal, intermediate and ventral domains within zebrafish pharyngeal arches. *Development* **137**, 2507-2517.
Tucker, A. S., Al Khamis, A. and Sharpe, P. T. (1998). Interactions between Bmp-4 and Msx-1 act to restrict gene expression to odontogenic mesenchyme. *Dev. Dyn.* **212**, 533-539.
Walker, M. B., Miller, C. T., Coffin Talbot, J., Stock, D. W. and Kimmel, C. B. (2006). Zebrafish furin mutants reveal intricacies in regulating Endothelin1 signaling in craniofacial patterning. *Dev. Biol.* **295**, 194-205.
Walker, M. B., Miller, C. T., Swartz, M. E., Eberhart, J. K. and Kimmel, C. B. (2007). phospholipase C, beta 3 is required for Endothelin1 regulation of pharyngeal arch patterning in zebrafish. *Dev. Biol.* **304**, 194-207.
Wall, N. A. and Hogan, B. L. (1995). Expression of bone morphogenetic protein-4 (BMP-4), bone morphogenetic protein-7 (BMP-7), fibroblast growth factor-8 (FGF-8) and sonic hedgehog (SHH) during branchial arch development in the chick. *Mech. Dev.* **53**, 383-392.
Wise, S. B. and Stock, D. W. (2010). bmp2b and bmp4 are dispensable for zebrafish tooth development. *Dev. Dyn.* **239**, 2534-2546.
Wozney, J. M., Rosen, V., Celeste, A. J., Mitsock, L. M., Whitters, M. J., Kriz, R. W., Hewick, R. M. and Wang, E. A. (1988). Novel regulators of bone formation: molecular clones and activities. *Science* **242**, 1528-1534.
Yanagisawa, H., Clouthier, D. E., Richardson, J. A., Charite, J. and Olson, E. N. (2003). Targeted deletion of a branchial arch-specific enhancer reveals a role of dHAND in craniofacial development. *Development* **130**, 1069-1078.
Zuniga, E., Stellabotte, F. and Crump, J. G. (2010). Jagged-Notch signaling ensures dorsal skeletal identity in the vertebrate face. *Development* **137**, 1843-1852.